Int J Adv Manuf Technol (1999) 15:546–553


The International Journal of
Advanced
Manufacturing
Technology

# Analyses of Drill Flute and Cutting Angles

Kaichun Ren[1] and Jun Ni[2]

[1]Mechanical Engineering College, Shanghai Jiaotong University, PR China; and [2]S. M. Wu Manufacturing Research Center, The University of Michigan, Ann Arbor, USA

*The analysis of drill cutting angles is important for the design of high-performance drill geometry. The cutting angles along the cutting edge of a drill are determined by the combination of its flute and flank surfaces. This paper examines the analysis of both flute and flank surface models and the evaluation of drill cutting angles. A new mathematical model for an arbitrary drill flute face is developed by sweeping the polynomial representation of the flute cross-sectional curve along the drill axis, with a helical movement. On the basis of the quadratic flank face, a relationship between the grinding and the geometrical design parameters of the flank face is also established. The vector analysis method is employed for the analysis of the cutting angles for various drill geometries. A comparison of the analytical results with the actual measured cutting angles of an example drill has shown that the average error is less than 5%.*

**Keywords:** Cutting angle; Drill; Flank surface; Flute surface

## 1. Introduction

Drill performance is significantly affected by its cutting angles, such as the relief and rake angles, along the entire drill cutting edges. Researchers over the past few decades have tried to optimise cutting angles for better drill performance by modifying drill geometry. Cutting edges are formed by the intersection of the flank and flute faces. Their shapes and orientations, with respect to the drill axis, greatly influence the design of the drills.

Most flute contour analyses were performed with the assumption that the primary cutting edge is a straight line [1–4]. However, many commercial drills are no longer confined to straight cutting edges owing to the better cutting performance of curved cutting edges over straight ones. Although some researchers [5,6] have analysed flutes by sweeping the cross-section, the analysis was still incomplete and inaccurate because of the assumption that the primary cutting edge of a conventional drill lies in a plane parallel to the drill axis. This assumption is only suitable in limited cases. In addition, the researchers did not provide a complete flute face model.

Recently, drills with various flute shapes have been developed for different drilling applications. Many of these flute contours have been developed by the trial-and-error approach. Thus, no theoretical models are available to represent these flute contours. In this paper, an accurate flute model based on the measurement of the drill cross-section is introduced. The flute model uses the polynomial representation of the drill cross-section and the sweeping of the cross-section curve with a helical movement around the drill axis. This paper also develops an analytical method for deriving drill cutting angles using vector analyses.

Section 2 presents the developed flute model. Since the drill cutting angles are formed by both the drill flute and drill flank surface, Section 3 will describe the quadratic drill flank surface models. Because the quadratic flank surface models are expressed in terms of grinding parameters, it is desirable to define the relationship between drill grinding and the geometrical design parameters. Section 4 will introduce the vector analysis method for cutting angle analysis, although the developed method is suitable for arbitrary drill design, Section 5 selects a spilt-point drill design as an example to show the comparative results between the analysis and actual measurement of cutting angles for a spilt-point drill.

## 2. Mathematical Models of Flute Geometry

The drill flute is an essential component of a drill body structure. Its shape and position affect the cutting performance of the drill, and are very closely related to the design of the grinding wheel shape for the flute generation. When a certain type of cross-section and helix angle are selected, the flute face can be represented by the helical motion of the initial cross-section. By rotating the cross-section of a drill around and down its *z*-axis simultaneously [1], an unpointed blank drill with a helix flute face is formed, as shown in Fig. 1.

*Correspondence and offprint requests to*: Dr Jun Ni, Department of Mechanical Engineering and Applied Mechanics, University of Michigan, 3424 G. G. Brown, Ann Arbor, MI 48109-2125, USA. E-mail: junni@umich.edu

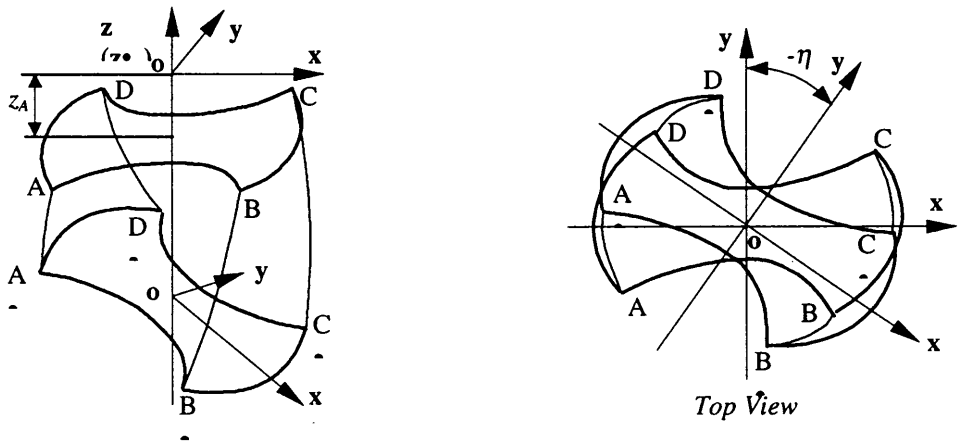


**Fig. 1.** Model of flute for two-flute drill.

**Table 1.** Results of statistical fitting of a flute cross-sectional curve.

| Statistic | *n*=5 (order) | *n*=8 (order) | *n*=12 (order) |
|---|---|---|---|
| $e_{min}$ (min residual | –0.080 | –0.053 | –0.028 |
| $e_{max}$ (max residual) | 0.109 | 0.050 | 0.021 |
| $\sigma$ (standard deviation of residual) | 0.051 | 0.026 | 0.011 |
| $\gamma^2$ (correlation coefficient) | 0.990 | 0.997 | 1.000 |

Here, **o-xyz** is the original coordinate, **o′-x′y′z′** is the rotating coordinate, and $\eta$ is the rotating angle. The model development for a flute face involves the following three steps.

### 2.1 Polynomial Representation of the Flute Cross-Sectional Curve

The flute curve on a cross-section can be approximated as a polynomial curve. Suppose that the equation of the flute curve takes the form:

$$R(x,y) = y - \sum_{i=0}^{n} b_i x^i = 0 \tag{1}$$

The coefficients $b_i (i=0,1,2,\ldots,n)$ must be determined from a series of data $(x_j,y_j)$ $(j=1,2,\ldots,m)$ measured along the flute cross-sectional curve:

$$x \quad x_1 \quad x_2 \quad \cdots \quad x_j \quad \cdots \quad x_m$$

$$y \quad y_1 \quad y_2 \quad \cdots \quad y_j \quad \cdots \quad y_m$$

In other words, the coefficients $b_i$ can be obtained from the following equations:

$$\begin{cases} \sum_{j=1}^{m} y_j - \sum_{i=0}^{n} b_i \sum_{j=1}^{m} x_j^i = 0 \\ \sum_{j=1}^{m-1} y_j - \sum_{i=0}^{n} b_i \sum_{j=1}^{m-1} x_j^i = 0 \\ \vdots \\ \sum_{j=1}^{m-n} y_j - \sum_{i=0}^{n} b_i \sum_{j=1}^{m-n} x_j^i = 0 \end{cases} \tag{2}$$

Usually $m>n$. The selection of the order $n$ depends on the shape of the flute curve on the cross-section. An example is given for fitting a group of flute curve data $(m=80)$ on the cross-section by using Eq. (2), as shown in Table 1 and Fig. 2. When $n$=12, the flute curve can be fitted very well. When $n>12$, $\sigma$ has almost no improvement.

### 2.2 Positioning of the Flute Curve

Because the fitted flute curve is located at an arbitrary position about the drill axis (z-axis), this curve must be rotated by a certain angle about the drill axis in order to make the point $A$ $(x_A,y_A,z_A)$ (see Fig. 3) at the outer corner fall onto the flute curve. The point $A$ is on both the flank and the rake faces. Its location influences the shape of the cutting lip. Generally, it can be assumed that the coordinates $x_A$ and $y_A$ of the point $A$ are located approximately at the following position:

$$\begin{cases} x_A = \dfrac{\sqrt{(D_d^2 - w_b^2)}}{2} \\ y_A = \dfrac{w_b}{2} \end{cases} \tag{3}$$

where $D_d$ is the drill diameter, and $w_b$ is the web thickness. The term $z_A$ can be obtained from Eq. (11).

Supposing the angle of rotation is $\varepsilon$, the equation of the flute curve becomes:

$$R(x',y') = y' - \sum_{i=0}^{n} b_i x'^i = 0 \tag{4}$$

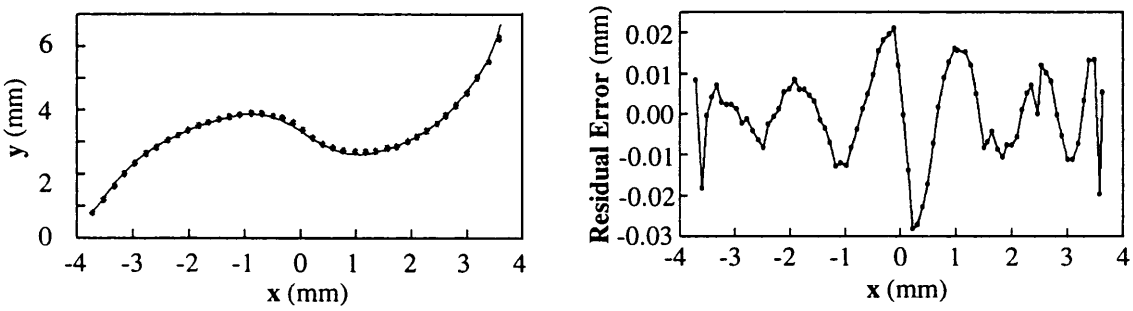


**Fig. 2.** Polynomial representation of flute cross-sectional curve and its residual error (order = 12).

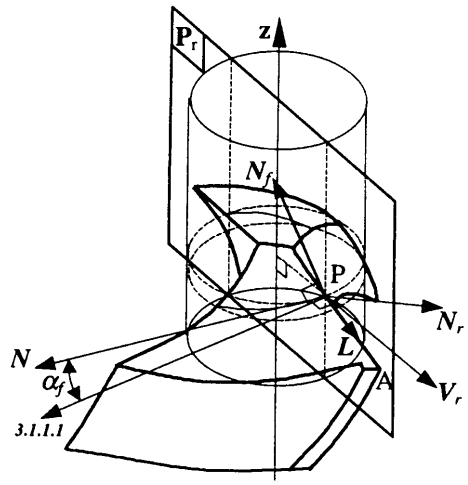


**Fig. 3.** Definition of relief angle.

where $x'$ and $y'$ satisfy the following equation:

$$\begin{pmatrix} x' \\ y' \end{pmatrix} = \begin{pmatrix} \cos\varepsilon & \sin\varepsilon \\ -\sin\varepsilon & \cos\varepsilon \end{pmatrix} \begin{pmatrix} x \\ y \end{pmatrix} \tag{5}$$

Hence, Eq. (4) becomes:

$$R(x,y) = x\sin\varepsilon - y\cos\varepsilon + \sum_{i=0}^{n} b_i(x\cos\varepsilon + y\sin\varepsilon)^i = 0 \tag{6}$$

Replacing $x$ and $y$ with $x_A$ and $y_A$ in Eq. (3), we can calculate the value of the angle $\varepsilon$.

### 2.3 Sweeping of the Flute Curve

After the cross-section sweeps down the z-axis from *ABCD* in the **o-xyz** coordinate system to *A′B′C′D′* in the **o′-x′y′z′** coordinate system (see Fig. 1), the flute surface is formed. The corresponding equation can be obtained from Eq. (6):

$$\begin{cases} R(x',y') = x'\sin\varepsilon - y'\cos\varepsilon + \sum_{i=0}^{n} b_i(x'\cos\varepsilon + y'\sin\varepsilon)^i = 0 \\ z = z_A + \dfrac{T_f}{2\pi}\eta = z_A + \dfrac{D_d}{2\tan\beta}\,\eta \end{cases} \tag{7}$$

where $T_f$ is the lead of the right-hand helix, $\beta$ is the helix angle, and $z_A$ is the coordinate of the point *A*. From Eqs (5) and (7), it yields:

$$\begin{aligned} R(x,y,z) &= (x\cos(\Delta_z\chi) + y\sin(\Delta_z\chi))\sin\varepsilon \\ &+ (x\sin(\Delta_z\chi) - y\cos(\Delta_z\chi))\cos\varepsilon + \sum_{i=0}^{n} b_i((x\cos(\Delta_z\chi) \\ &+ y\sin(\Delta_z\chi))\cos\varepsilon - (x\sin(\Delta_z\chi) - y\cos(\Delta_z\chi))\sin\varepsilon)^i = 0 \end{aligned} \tag{8}$$

where,

$$\chi = 2\pi/T_f = 2\tan\beta/D_d$$
$$\Delta_z = z - z_A$$

The above is the equation of a flute face.

## 3. Mathematical Models of Flank Faces

To date, a large number of different drill points are commercially available. Despite the wide variety, there are only a few types of flank faces for current drill points, owing to manufacturing limitations. The following subsections will present the equations of the flank faces and describe the relationship between the grinding parameters that are used for the surface model and the geometric design parameters that are commonly used by tool engineers in the analysis and design of drills.

### 3.1 Equation of the Flank Face

For various drill points, the flank face or the main part of the flank face is generally modelled by one of the basic surfaces, e.g. hyperbolic, ellipsoidal, conical, cylindrical or planar. All of the above surfaces can be represented by a generalised rotary quadratic equation [3]:

$$\frac{x^{*2}}{a^2} + \frac{y^{*2}}{a^2} + \delta\frac{z^{*2}}{c^2} = 1 \tag{9}$$

where, $a$, $c$, and $\delta$ are parameters that decide the shape of a quadratic surface. Conical, ellipsoidal, hyperboloidal, and cylindrical grinding models are shown in Fig. 4. After the transformation from the coordinate system **o*-x*y*z*** to the drill coordinate system **o-xyz**, the mathematical model of a drill flank is obtained as:

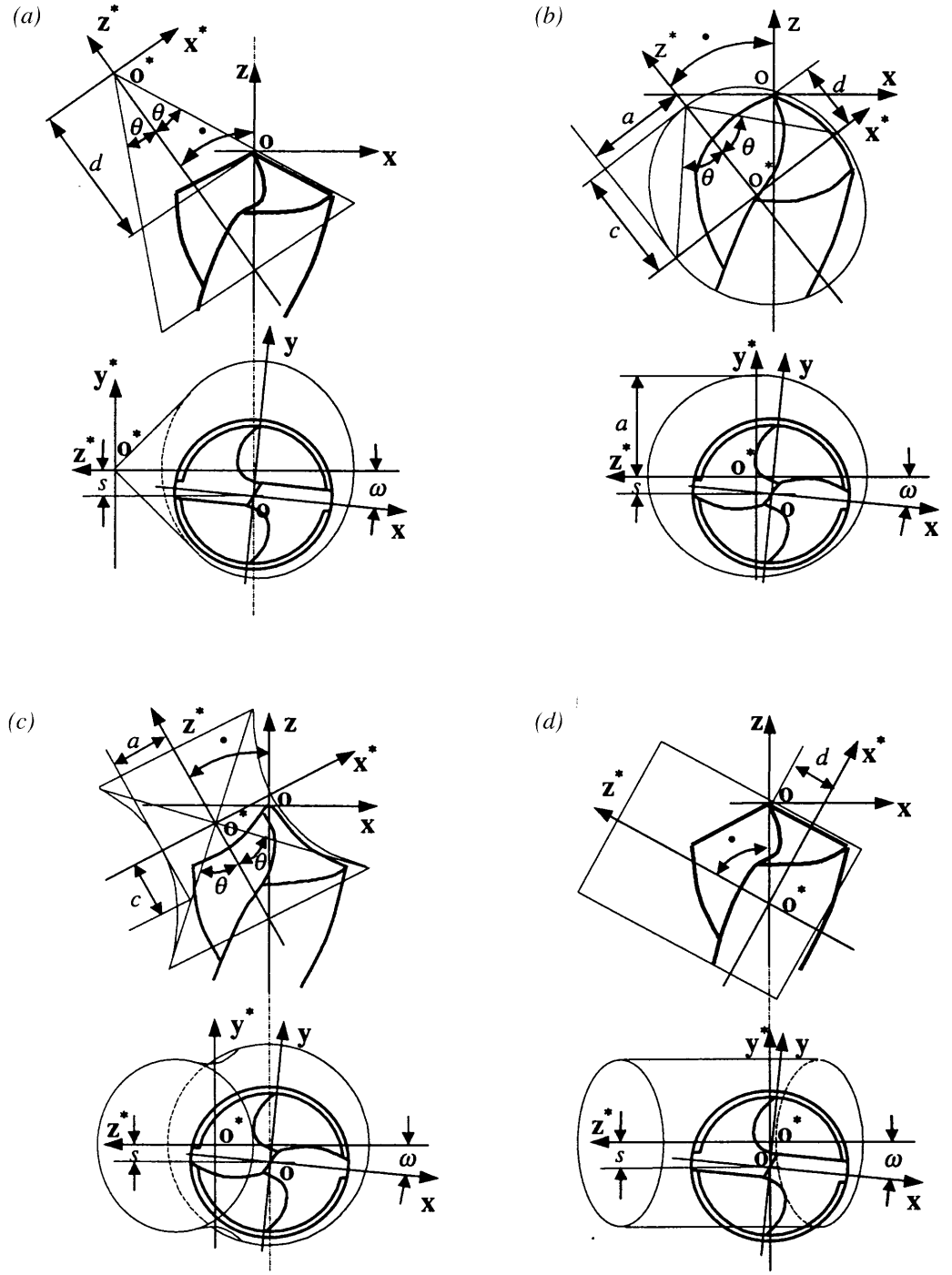


**Fig. 4.** Models for quadratic drill points. (*a*) Conical model. (*b*) Ellipsoidal model. (*c*) Hyperboloidal model. (*d*) Cylindrical model.

$$\frac{1}{a^2}\left((x\cos\omega + y\sin\omega)\cos\varphi + z\sin\varphi + \sqrt{\left(a^2 - \delta\frac{a^2}{c^2}d^2 - s^2\right)}\right)^2$$

$$+ \frac{1}{a^2}\left((x\sin\omega - y\cos\omega) + s\right)^2$$

$$+ \frac{\delta}{c^2}(z\cos\varphi - (x\cos\omega + y\sin\omega)\sin\varphi - d)^2 = 1 \qquad (10)$$

This is a general expression of a drill flank with a rotary quadratic surface, and can be expressed in the more generalised form:

$$F(x,y,z) = E_1x^2 + E_2y^2 + E_3z^2 + E_4xy + E_5yz + E_6zx$$

$$+ E_7x + E_8y + E_9z = 0 \qquad (11a)$$

where,

$$\begin{cases} E_1 = \sin^2\omega + \cos^2\omega\left(\cos^2\varphi + \delta\dfrac{a^2}{c^2}\sin^2\varphi\right) \\ E_2 = \cos^2\omega + \sin^2\omega\left(\cos^2\varphi + \delta\dfrac{a^2}{c^2}\sin^2\varphi\right) \\ E_3 = \cos^2\varphi\left(\tan^2\varphi + \delta\dfrac{a^2}{c^2}\right) \\ E_4 = -\sin 2\omega\sin^2\varphi\left(1 - \delta\dfrac{a^2}{c^2}\right) \\ E_5 = \sin\omega\sin 2\varphi\left(1 - \delta\dfrac{a^2}{c^2}\right) \\ E_6 = \cos\omega\sin 2\varphi\left(1 - \delta\dfrac{a^2}{c^2}\right) \\ E_7 = 2\left(s\sin\omega + \cos\omega\left(\cos\varphi\sqrt{\left(a^2 - \delta\dfrac{a^2}{c^2}d^2 - s^2\right)} + \delta\dfrac{a^2}{c^2}d\sin\varphi\right)\right) \\ E_8 = 2\left(-s\cos\omega + \sin\omega\left(\cos\varphi\sqrt{\left(a^2 - \delta\dfrac{a^2}{c^2}d^2 - s^2\right)} + \delta\dfrac{a^2}{c^2}d\sin\varphi\right)\right) \\ E_9 = 2\left(\sin\varphi\sqrt{\left(a^2 - \delta\dfrac{a^2}{c^2}d^2 - s^2\right)} - \delta\dfrac{a^2}{c^2}d\cos\varphi\right) \end{cases} \tag{11b}$$

Equation (11*a*) describes one side of the flank. Symmetrically, the other side of the flank can be obtained by substituting $x$ with $-x$ and $y$ with $-y$ in Eq. (11*a*):

$$F'(x,y,z) = E_1x^2 + E_2y^2 + E_3z^2 + E_4xy - E_5yz - E_6zx - E_7x - E_8y + E_9z = 0 \tag{12}$$

For different combinations and values of parameters $a$, $c$, and $\delta$, various surfaces can be obtained from Eqs (10) or (11):

*Conical flank* $\delta = -1$, $a \to 0$, $c \to 0$, and set $\tan\theta = a/c$
*Hyperboloidal flank* $\delta = -1$
*Ellipsoidal flank* $\delta = 1$
*Cylindrical flank* $\delta = 0$

## 3.2 Relationship between Geometrical Design and Grinding Parameters

Equations (11) and (12) are described only with the grinding parameters. Generally, a drill is designed in terms of its geometry parameters. Therefore, the corresponding relationship between the geometrical design parameters and the grinding parameters must be established to achieve the conversion between the two groups of parameters. The following derivations are modified from the results of Lin et al. [7].

### 3.2.1 Semi-Point Angle $\rho$

A cutting edge is formed by the intersection of the flank face $F(x,y,z)$ and the rake face $R(x,y,z)$. If the cutting edges are curved, the drill semi-point angle, $\rho$, will vary along the cutting edges. Generally, the drill nominal semi-point angle $\rho$ is specified at the outer corner point $A$ $(x_A,y_A,z_A)$, and is defined as the acute angle between the tangent to the projection of the cutting lip at the outer corner point $A$ and the drill axis on the **x**,**z**-plane. Figure 5 illustrates the drill semi-point angle $\rho$, that is:

$$\rho = \tan^{-1}\left.\frac{\dfrac{\partial F}{\partial z}\dfrac{\partial R}{\partial y} - \dfrac{\partial F}{\partial y}\dfrac{\partial R}{\partial z}}{\dfrac{\partial F}{\partial x}\dfrac{\partial R}{\partial y} - \dfrac{\partial F}{\partial y}\dfrac{\partial R}{\partial x}}\right|_A = \tan^{-1}\left.\frac{N_{fz}\,N_{ry} - N_{fy}\,N_{rz}}{N_{fx}\,N_{ry} - N_{fy}\,N_{rx}}\right|_A \tag{13}$$

where $N_{fx}$, $N_{fy}$,$N_{fz}$ and $N_{rx}$, $N_{ry}$, $N_{rz}$ will be derived in Eqs (26) and (31).

### 3.2.2 Chisel Edge Angle $\psi$

The chisel edge is the intersection of the two symmetrical flanks, $F(x,y,z)$ and $F'(x,y,z)$. It passes through the drill point centre and can be a spatial curve when the flanks are common quadratic surfaces or a straight line when both flanks are planes. As shown in Fig. 5, the chisel edge angle $\psi$ is the acute angle between the tangent to the projection of the chisel edge onto the plane perpendicular to the drill axis at the point centre and the **x**-axis.

$$\psi = \tan^{-1}\left(\frac{\partial y}{\partial x}\right)_o = \tan^{-1}\left(-\frac{\partial F/\partial x}{\partial F/\partial y}\right)_o \tag{14}$$

From Eq. (11), it yields

$$\begin{cases} \left.\dfrac{\partial F}{\partial x}\right|_o = (2E_1x + E_4y + E_6z + E_7)_{x=y=z=0} = E_7 \\ \left.\dfrac{\partial F}{\partial y}\right|_o = (2E_2y + E_4x + E_5z + E_8)_{x=y=z=0} = E_8 \end{cases}$$

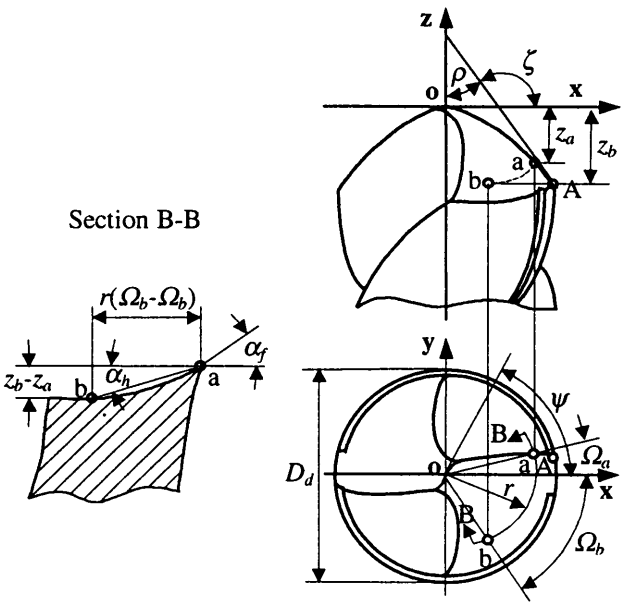


**Fig. 5.** Definition of the drill semi-point angle $\rho$ and heel clearance angle $\alpha_h$.

Therefore, Eq. (14) becomes:

$$\psi = \tan^{-1}\left(-\frac{E_7}{E_8}\right) \tag{15}$$

#### 3.2.3 Relief Angle $\alpha_{fA}$

In Section 4, an analysis of the relief angle $\alpha_f$ is presented in detail. Substituting the outer corner point $A(x_A,y_A,z_A)$ into Eq. (29) yields:

$$\alpha_{fA} = \cos^{-1}\left(\frac{\sqrt{(x^2+y^2)}N_{fz}}{\sqrt{((x^2+y^2)N_{fz}^2 + (yN_{fx} - xN_{fy})^2)_A}}\right) \tag{16}$$

#### 3.2.4 Heel Clearance Angle $\alpha_h$

As illustrated in Fig. 5, the heel clearance angle $\alpha_h$ is an acute angle whose amplitude determines the extent of inclination of the relief face close to the heel flute area. Its tangent is equal to the axial drop between a point on the cutting edge and a specified point on the flank at the same radius $r$ divided by the circumferential distance between the two points. Suppose the point $a$ is on the cutting edge and the point $b$ is on the flank at the same radial distance $r$. The heel clearance angle $\alpha_h$ at the point $b$ is defined by:

$$\alpha_{h-b} = \tan^{-1}\frac{z_a - z_b}{\frac{2\pi r}{360}(\grave{U}_a + \grave{U}_b)} = \tan^{-1}\frac{180(z_a - z_b)}{\pi r(\grave{U}_a + \grave{U}_b)} \tag{17}$$

The heel clearance angle $\alpha_h$ at a special point $b$ close to the heel corner, $r = D_d/2$ and $\Omega_b = 60°$, can be written as:

$$\alpha_{h-b} = \tan^{-1}\frac{360(z_a - z_b)}{\pi D_d(\grave{U}_a + 60)} \tag{18}$$

where,

$$\grave{U}_a = \sin^{-1}\frac{w_b/2}{D_d/2} = \sin^{-1}\frac{w_b}{D_d}$$

$$x_a = x_A$$

$$y_a = y_A$$

$$x_b = \sqrt{\left(x_A^2 + y_A^2\right)}\cos\grave{U}_b = \sqrt{\left(x_A^2 + y_A^2\right)}\cos 60°$$

$$y_b = \sqrt{\left(x_A^2 + y_A^2\right)}\sin\grave{U}_b = \sqrt{\left(x_A^2 + y_A^2\right)}\sin 60° \tag{19}$$

$z_a$ and $z_b$ can be alculated by substituting Eq. (19) into Eqs (10) or (11).

## 4. Cutting Angle Analysis

The study of the cutting angles of drills is of importance in the design and analysis of drills. Many other models and analyses, such as the calculation of force, temperature, wear, and chip ejection, are based on cutting angle analysis. In this section, general formulae for rake and relief angle calculation are derived.

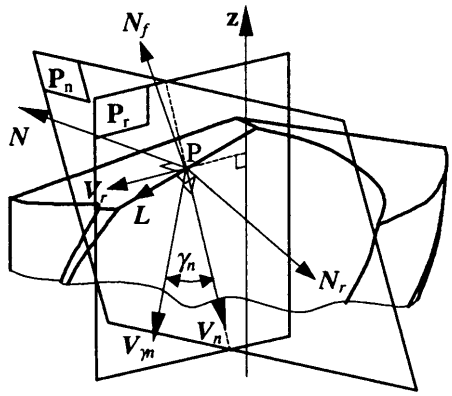


**Fig. 6.** Definition of rake angle.

### 4.1 Cutting Lips

One of the key components of the drill geometry is the cutting lip that is associated with the cutting angles. Cutting lips are formed by the intersection of the flank and rake faces. Suppose that the equations of the flank and rake faces are $F(x,y,z)$=0 and $R(x,y,z)$=0, respectively. The equation of the cutting lip can be obtained by solving the simultaneous equations:

$$\begin{cases} F(x,y,z) = 0 \\ R(x,y,z) = 0 \end{cases} \tag{20}$$

$F(x,y,z)$ and $R(x,y,z)$ are nonlinear and implicit. A numerical method has to be applied for Eq. (20) because it is normally impossible to obtain its algebraic explicit solution. Any arbitrary point $P(x,y,z)$ (see Figs 3 and 6) on the cutting lip should satisfy the above equation.

For the flank face $F(x,y,z) = 0$, the normal vector $\mathbf{N}_f(N_{fx}, N_{fy}, N_{fz})$ of a plane tangent to this surface is:

$$\mathbf{N}_f = N_{fx}\mathbf{i} + N_{fy}\,\mathbf{j} + N_{fz}\,\mathbf{k} = \frac{\partial F}{\partial x}\mathbf{i} + \frac{\partial F}{\partial y}\mathbf{j} + \frac{\partial F}{\partial z}\mathbf{k} \tag{21}$$

and for the rake face $R(x,y,z) = 0$, the normal vector $\mathbf{N}_r(N_{rx}, N_{ry}, N_{rz})$ of a plane tangent to this surface can be represented by:

$$\mathbf{N}_r = N_{rx}\mathbf{i} + N_{ry}\mathbf{j} + N_{rz}\mathbf{k} = \frac{\partial R}{\partial x}\mathbf{i} + \frac{\partial R}{\partial y}\mathbf{j} + \frac{\partial R}{\partial z}\mathbf{k} \tag{22}$$

Then the tangent vector $\mathbf{L}(L_x,L_y,L_z)$ of the cutting lip at the point $P$ satisfies the formula:

$$\mathbf{L} = \mathbf{N}_r \times \mathbf{N}_f = \begin{vmatrix} \mathbf{i} & \mathbf{j} & \mathbf{k} \\ N_{rx} & N_{ry} & N_{rz} \\ N_{fx} & N_{fy} & N_{fz} \end{vmatrix} \tag{23}$$

### 4.2 Relief Angle Analysis

The relief angle is one of the important factors for improving drill performance. A proper relief angle means that:

1. The clearance is large enough to suit the specified feedrate without touching the newly cut surface on the bottom.

2. There is enough material in the drill flank to conduct heat and to ensure necessary strength.

In this section a mathematical formula of the relief angle, relating to the drill geometry parameters, is derived. The relief angle $\alpha_f$ at the point $P(x,y,z)$ along the cutting lip is the angle between the direction vector $\mathbf{V}_{\alpha f}(V_{\alpha fx}, V_{\alpha fy}, V_{\alpha fz})$ and the normal vector $\mathbf{N}$ $(N_x, N_y, N_z)$ of the reference plane $\mathbf{P}_r$. $\mathbf{V}_{\alpha f}$ is perpendicular to the normal vector $\mathbf{N}_f$ and the reference vector $\mathbf{V}_r$, and $\mathbf{V}$ is perpendicular to the reference plane $\mathbf{P}_r$ as shown in Fig. 3. The plane $\mathbf{P}_r$ passes through the **z**-axis and the point $P$.

The reference vector $\mathbf{V}_r(V_{rx}, V_{ry}, V_{rz})$ on the reference plane $\mathbf{P}_r$ is:

$$\mathbf{V}_r = V_{rx}\mathbf{i} + V_{ry}\mathbf{j} + V_{rz}\mathbf{k} = x\mathbf{i} + y\mathbf{j} + 0\mathbf{k} \tag{24}$$

The direction vector $\mathbf{V}_{\alpha f}(V_{\alpha fx}, V_{\alpha fy}, V_{\alpha fz})$ is:

$$\mathbf{V}_{\acute{a}f} = \mathbf{V}_r \times \mathbf{N}_f = \begin{vmatrix} \mathbf{i} & \mathbf{j} & \mathbf{k} \\ V_{rx} & V_{ry} & V_{rz} \\ N_{fx} & N_{fy} & N_{fz} \end{vmatrix} = \begin{vmatrix} \mathbf{i} & \mathbf{j} & \mathbf{k} \\ x & y & 0 \\ N_{fx} & N_{fy} & N_{fz} \end{vmatrix} \tag{25}$$

The normal vector $\mathbf{N}_f$ at the point $P$ can be obtained from Eq. (11):

$$\begin{cases} N_{fx} = 2E_1x + E_4y + E_6z + E_7 \\ N_{fy} = 2E_2y + E_4x + E_5z + E_8 \\ N_{fz} = 2E_3z + E_5y + E_6x + E_9 \end{cases} \tag{26}$$

Then the relief angle along the cutting lip is:

$$\alpha_f = \cos^{-1}\frac{\mathbf{N}\cdot\mathbf{V}_{\acute{a}f}}{|\mathbf{N}\|\mathbf{V}_{\acute{a}f}|} = \cos^{-1}\frac{V_xV_{\alpha fx} + V_yV_{\alpha fy} + V_zV_{\alpha fz}}{\sqrt{(V_x^2+V_y^2+V_z^2)}\ \sqrt{(V_{\alpha fx}^2+V_{\alpha fy}^2+V_{\alpha fz}^2)}} \tag{27}$$

Because

$$\mathbf{N} = N_x\mathbf{i} + N_y\mathbf{j} + N_z\mathbf{k} = y\mathbf{i} - x\mathbf{j} + 0\mathbf{k} \tag{28}$$

Substituting for $\mathbf{V}$ and $\mathbf{V}_{\alpha f}$ into Eq. (27) yields:

$$\alpha_f = \cos^{-1}\frac{\sqrt{(x^2+y^2)}\,N_{fz}}{\sqrt{((x^2+y^2)N_{fz}{}^2 + (yN_{fx} - xN_{fy})^2)}} \tag{29}$$

### 4.3 Rake Angle Analysis

Like the relief angle, the normal rake angle $\gamma_n$ is a function of the position along the cutting lip. For any point $P(x,y,z)$ on the cutting lip, there are two datum planes: the normal plane $\mathbf{P}_n$ and the reference plane $\mathbf{P}_r$. The plane $\mathbf{P}_n$ is perpendicular to the tangent line $\mathbf{L}$ $(L_x, L_y, L_z)$ of the cutting lip at the point $P$, and the plane $\mathbf{P}_r$ passes through the **z**-axis and the point $P$. The rake angle vector $\mathbf{V}_{\gamma n}(V_{\gamma nx}, V_{\gamma ny}, V_{\gamma nz})$ is along the intersection line of the plane $\mathbf{P}_n$ and the tangent plane of the flute face at the point $P$. The reference vector $\mathbf{V}_n(V_{nx}, V_{ny}, V_{nz})$ is along the intersection line of the plane $\mathbf{P}_n$ and the reference plane $\mathbf{P}_r$. The normal rake angle $\gamma_n$ is defined as an angle between the vector $\mathbf{V}_{\gamma n}$ and the vector $\mathbf{V}_n$ as shown in Fig. 6.

The rake angle vector $\mathbf{V}_{\gamma n}(V_{\gamma nx}, V_{\gamma ny}, V_{\gamma nz})$ is:

$$\mathbf{V}_{\tilde{a}n} = \mathbf{N}_r \times \mathbf{L} = \begin{vmatrix} \mathbf{i} & \mathbf{j} & \mathbf{k} \\ N_{rx} & N_{ry} & N_{rz} \\ L_x & L_y & L_z \end{vmatrix} \tag{30}$$

For the primary cutting edge of a drill, the flute is the rake face. The normal vector $\mathbf{N}_r$ at the point $P$ can be obtained from Eqs (8) and (22):

$$\begin{cases} N_{rx} = \cos(\Delta_z\chi)\sin\varepsilon + \sin(\Delta_z\chi)\cos\varepsilon + (\cos(\Delta_z\chi)\cos\varepsilon - \sin(\Delta_z\chi)\sin\varepsilon) \\ \sum_{i=1}^{n} \mathbf{i}b_i((x\cos(\Delta_z\chi) + y\sin(\Delta_z\chi))\cos\varepsilon - (x\sin(\Delta_z\chi) - y\cos(\Delta_z\chi))\sin\varepsilon)^{i-1} \\ N_{ry} = \sin(\Delta_z\chi)\sin\varepsilon - \cos(\Delta_z\chi)\cos\varepsilon + (\sin(\Delta_z\chi)\cos\varepsilon + \cos(\Delta_z\chi)\sin\varepsilon) \\ \sum_{i=1}^{n} \mathbf{i}b_i((x\cos(\Delta_z\chi) + y\sin(\Delta_z\chi))\cos\varepsilon - (x\sin(\Delta_z\chi) - y\cos(\Delta_z\chi))\sin\varepsilon)^{i-1} \\ N_{rz} = -\chi(x\sin(\Delta_z\chi) - y\cos(\Delta_z\chi))\sin\varepsilon + \chi(x\cos(\Delta_z\chi) + y\sin(\Delta_z\chi))\cos\varepsilon \\ -\chi((x\sin(\Delta_z\chi) - y\cos(\Delta_z\chi))\cos\varepsilon + (x\cos(\Delta_z\chi) + y\sin(\Delta_z\chi))\sin\varepsilon) \\ \sum_{i=1}^{n} b_i((x\cos(\Delta_z\chi) + y\sin(\Delta_z\chi))\cos\varepsilon - (x\sin(\Delta_z\chi) - y\cos(\Delta_z\chi))\sin\varepsilon)^{i-1} \end{cases} \tag{31}$$

The reference vector $\mathbf{V}_n(V_{nx}, V_{ny}, V_{nz})$ is:

$$\mathbf{V}_n = \mathbf{L} \times \mathbf{N} = \begin{vmatrix} \mathbf{i} & \mathbf{j} & \mathbf{k} \\ L_x & L_y & L_z \\ N_x & N_t & N_z \end{vmatrix} = \begin{vmatrix} \mathbf{i} & \mathbf{j} & \mathbf{k} \\ L_x & L_y & L_z \\ y & -x & 0 \end{vmatrix} \tag{32}$$

Then the normal rake angle can be obtained:

$$\gamma_n = \cos^{-1}\frac{\mathbf{V}_{\gamma n}\cdot\mathbf{V}_n}{|_{\gamma n}\|\mathbf{V}_n|} = \cos^{-1}\frac{V_{\gamma nx}V_{nx} + V_{\gamma ny}V_{ny} + V_{\gamma nz}V_{nz}}{\sqrt{(V_{\gamma nx}^2+V_{\gamma ny}^2+V_{\gamma nz}^2)}\ \sqrt{(V_{nx}^2+V_{ny}^2+V_{nx}^2)}} \tag{33}$$

**Table 2.** Fitted coefficients $b_i$ ($n$=12) of a flute curve on the cross-section.

| | |
|---|---|
| $b_0$ | –0.6906115 |
| $b_1$ | –0.0562371 |
| $b_2$ | 0.4108830 |
| $b_3$ | –0.0590901 |
| $b_4$ | –0.1370808 |
| $b_5$ | 0.0393022 |
| $b_6$ | 0.0373205 |
| $b_7$ | –0.0029054 |
| $b_8$ | –0.005149 |
| $b_9$ | –0.0005039 |
| $b_{10}$ | 0.0002485 |
| $b_{11}$ | 0.0000624 |
| $b_{12}$ | 0.0000042 |

## 5. Comparison of the measured and calculated angles

Equations (29) and (33) for the cutting angle calculation are complicated. Therefore, a program was developed for calculating the distribution of relief and rake angles. An example is given to validate the formulae.

From the data used for fitting the flute curve on the cross-section in Section 2, the coefficients $b_i$ of Eq. (8) are calculated and shown in Table 2. Based on the data of the parameters of a split drill with conical flank in Table 3, the distribution of

**Table 3.** Geometrical parameters of a split drill.

| $D_d$ Diameter (mm) | $w_b$ Web thickness (mm) | ρ Semi-point angle (deg.) | β Helix angle of flute (deg.) | $\alpha_c$ Relief angle on cutter corner (deg.) | $\alpha_h$ Heel angle (deg.) | ψ Chisel edge angle (deg.) |
|---|---|---|---|---|---|---|
| 8.5 | 2.7 | 170 | 26.05 | 15 | 18 | 55 |

the cutting edges is shown in Fig. 7. The calculated and measured values of the cutting angles agree with each other very well. The average error is less than 5%.

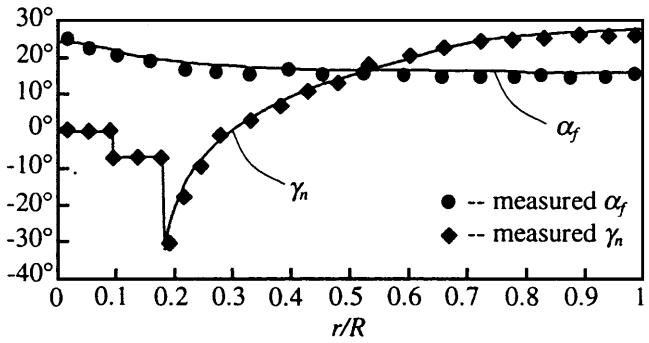


**Fig. 7.** Distribution of relief and rake angles (solid lines are calculated values).

## 6. Conclusion

This paper presents an analysis of drill cutting angles along the cutting edges of a drill. To facilitate the analysis, both drill flank and flute surface models are necessary. For drill flank surface representation, conventional quadratic surface models have been adopted with some minor modifications. A new drill flute face model is introduced with the use of a polynomial representation of an arbitrary flute cross-sectional curve and a sweeping helix motion along the drill body axis. In the evaluation of drill cutting angles, the vector analysis method is used to derive generalised solutions. As an example, a split drill is measured and evaluated with the presented method. The results from both the measured rake and relief angle distribution and the analytical calculation have shown a good agreement. These models for cutting angle analysis can serve as a fundamental basis for other drilling process modelling such as the prediction of force, temperature, chip formation, and ejection.

### References

1. D. F. Galloway, “Some experiments on the influence of various factors on drill performance”, Transactions ASME, 79, pp. 191–231, 1957.
2. S. Fujii, M. F. Devries and S. M. Wu, “An analysis of drill geometry for optimum drill design by computer, Parts I and II, Drill geometry analysis; Computer-aided design”, Journal of Engineering for Industry, Transactions ASME, Series B, 92, pp. 647–666, 1970.
3. W. D. Tsai and S. M. Wu, “A mathematical model for drill point design and grinding”, Journal of Engineering for Industry, 101(3), pp. 333–340, 1979.
4. H. T. Huang, C. I. Weng and C. K. Chen, “Analysis of clearance and rake angles along cutting edge for multifacet drill”, Journal of Engineering for Industry, 116(1), pp. 8–16, 1994.
5. Y. Wang, “Computer graphics presentation of drilling operations”, PhD thesis, The University of Michigan, 1990.
6. J.-L. Wang, J. Sha and J. Ni, “Further improvement of multifacet drills”, S. M. Wu Symposium, vol. 1, pp. 115–122, 1994.
7. C. Lin, S. K. Kang and K. F. Ehmann, “Helical micro-drill point design and grinding”, Journal of Engineering for Industry, 117(4), pp. 277–287, 1995.